Romanian Reports in Physics, Vol. 62, No. 3, P. 528–545, 2010

LASER INTERACTIONS WITH MATTER

Dedicated to the 50th LASER Anniversary
(LASERFEST-50)

RECENT PROGRESS IN THE THEORETICAL INVESTIGATION OF LASER-ATOM, LASER-PLASMA INTERACTIONS

V. STANCALIE[1], V. PAIS[1], A. MIHAILESCU[1], O. BUDRIGA[1], A. OPREA[1,2]

[1] *National Institute for Laser, Plasma and Radiation Physics, Department of Lasers, Atomistilor Str. 409, P.O.Box MG-36, RO- 077125 Magurele, Romania, E-mail: viorica.stancalie@inflpr.ro; vasile.pais@inflpr.ro, andreea.mihailescu@inflpr.ro, olimpia.budriga@inflpr.ro, andreea.oprea@inflpr.ro*

[2] *University of Buchares, Faculty of Physics, RO-077125 Magurele, Romania*

(Received May 25, 2010)

Abstract. This work discusses the non-perturbative method which has been used to study laser-atom interactions at high intensity. Separate account is given of relation between photon emission rate and ionization or recombination flux contributing to the opacity effects in high intensity laser-plasma interactions.

Key words: photoionisation, laser induced atomic processes, plasma opacity

1. INTRODUCTION

The study of laser-atom interactions at high intensities is an excited area of atomic physics related to fusion researches. Rapid advances in this domain have become possible due to the development, using the "Chirped Pulse Amplification" (CPA) scheme [1] of lasers capable of yielding intensities of the order exceeding the value corresponding to the atomic unit of electric field strength. Such laser fields are strong enough to complete with the Coulomb forces in controlling the electron dynamics in atomic systems. As a results, atoms and molecules in intense laser fields exhibit new properties which have been discovered via the study of multiphoton processes [2].These properties generate new behavior of bulk matter in intense laser fields, with wide ranging potential applications such as the study of ultra-fast phenomena, the development of high frequency (XUV and X-ray) lasers, the investigation of the properties of plasmas and condensed matter under extreme

conditions of temperature and pressure, and intense field control of atomic and molecular reactions. Over the last ten years, laser intensities have increased by four orders of magnitude, up to 10^{20} W cm^{-2} where relativistic effects in laser-atom interactions become important [3-6].

On the theoretical side, the development of supercomputers has made it possible to perform calculations of unprecedented complexity, which have led to the prediction of novel properties of atomic systems in strong laser fields.While dense matter is typically electrically neutral, the light pressure of these ultra-intense laser pulses can separate electrons from ions completely, thus generating huge space charge fields in which charged particles are accelerated [7-9]. Fast ignition entails assembly of compressed fuel followed by fast heating. Accurate understanding and interpretation of phenomena involves the knowledge of atomic and molecular processes dynamics in electromagnetic field. In the last years, with the development of new instruments and technology able to measure spectra in the X-UV region, this activity made an unexpected progress. In simple gas targets, this may lead to the "bubble" regime, in which an electron-void volume trailing a short laser pulse self-traps electrons and accelerates them to hundreds of MeV. Corresponding electron pulses are now observed by many groups. Guiding the laser pulse in capillaries, thus extending the acceleration distance, has led to the production of GeV electrons. At solid interfaces, the space charge fields accelerate ions to multi-MeV energies. These beams have been observed with remarkably low emittance, and much of the current discussion concentrates on how to make mono-energetic ion pulses. Recent theoretical works show that ultra-thin foils and clusters can be accelerated as a whole close to the velocity of light, with pushed electrons dragging all ions. [10]. Complementary to electron-void regions, one finds dense electron fronts moving with high relativistic velocities. These fronts may backscatter optical photons and convert them into X-rays. At steep surfaces, oscillating relativistic mirrors compress incident laser light into attosecond flashes, corresponding to high harmonic spectra. It looks feasible to even focus these flashes, thereby reaching intensities close to the Schwinger limit for pair production from the vacuum. It is the first time that we have a realistic option to achieve electric fields of the order of 10^{16} V cm^{-1} at which light significantly disturbs the vacuum.

In the presence of an intense laser field, atomic and molecular states are dressed in the continuum. This can promote a discrete state into a photoionization continuum. Such a process, referred to as a laser-induced continuum structure (LICS), has been studied by Knight [11] and Kylstra *et al.* [12]. A LICS creates a tunable 'pseudo-autoionizing resonance' of adjustable position and width. Shao *et al*. [13] also showed that it is possible to induce a LICS by exciting Rydberg states into the continuum. They have observed LICS in the ionization spectrum of sodium. Laser-induced degenerate states (LIDS) are different from LICS in that they involve two laser dressed atomic states. If for a particular laser frequency and

intensity, the dressed autoionizing state and the dressed ground state (LICS) are degenerate (have the same energy and width), they form what is called a LIDS. Pumping an atom from the ground state into an excited state with the help of a laser is usually performed by tuning the laser to resonance and waiting sufficiently long. This process can be understood in terms of a simple two-level model atom, in which the laser coupling induces Rabi oscillations of the population between the two states. In principle, population can be transferred to 100% by choosing the pulse length appropriately ~''π pulse''. Decay processes can be included in this model, for example the spontaneous decay, which destroys the coherence, but still allows at least 50% population transfer. When laser-induced ionization of the atom becomes important, however, in particular when the ionization rate of the upper level becomes comparable to the Rabi frequency, it is not evident that population can be transferred through Rabi oscillations.

Opacity issues are of crucial importance when modeling X-ray spectra from laser-plasmas.

Experimental and theoretical determinations of the radiative opacity have long been of interest. Many physical effects which have been treated approximately or ignored in theoretical models may affect the accuracy of opacity. Some discrepancies are supposed to be a consequence of line saturation effect. Method and codes exist for wide range of electron-impact excitation and ionization processes: the Convergent Close Coupling (CCC) theory and method is meant to be applicable at all energies for the major excitation and ionization processes [14]. The Plane-Wave Born (PWB) and first order many body perturbation theories (FOMBT) [15] and methods have also shown good agreement in some cases but very large differences for forbidden transitions in electron impact excitation. Resonances are not treated correctly by either PWB or FOMBT and require the use of the R-matrix method or of the CCC method. Excitation can be a direct process or a result of resonant dielectronic capture followed by autoionization leaving the target ion in an excited state. Resonant enhancements to the cross section are significant in optically-forbidden transitions and can dominate the direct contribution by an order of magnitude or more near threshold. Direct configuration interaction (CI) and indirect interactions with a common continuum have shown [16] to produce interference between nearby resonances and have a strong effect on the resonance contributions to the cross sections as calculated in the close coupling formulation. It has been found that the resonance structure is sensitive to the exact energies of the individual resonances.

Doubly excited states (resonances) offer a very suitable laser frequency regime within which to undertake investigative calculations has already attracted interest. The resonance regions have been studied in the context of multiphoton transitions. There have been several theoretical methods introduced to describe multiphoton processes in atoms. Of these calculations only those employing the R-matrix Floquet [20, 21] (RMF) method couple the field to the ion non-

perturbatively, and only those of Latinne *et al*. [22, 23] explicitly investigated the laser induced modification of doubly excited states, that is to say, the interplay of laser-induced degenerate states (LIDS). Specifically, the frequency and the intensity of the light field can be adjusted such that the energy and the width of the dressed ground state coincide with the energy and the width of the dressed autoionizing state. The motion of the complex energies in the complex plane as function of the field intensity for different frequencies and atomic parameters gives complementary information on the role of LIDS on resonances obtained by laser. It was shown that the rate of the 'ground' excited Rydberg state will first increase with the intensity and then exhibit a typical 'stabilisation', namely a decrease of the ionization rate with increasing intensity. The most interesting is the critical region where a crossing (or an avoiding crossing) occurs.

In the present work we focused on the Li-like ions interacting with an intense laser field. Aluminum material and presence of carbon in polymer target materials are of importance in laser irradiated cryogenically cooled pellet target design. There fore X-radiation emission study from aluminum and carbon material is important.

In general one associates double-resonant processes with processes induced by two lasers. In our work, instead of using a probe laser to reach a high-lying state in the continuum, this state is reached by choosing the energy of the incident electrons to be at resonance with the resonant state of the composite electron-atom system. An intense laser is then used to strongly couple the autoionizing state to another state. The advantage of such approach is that it allows flexibility: tuning the energy of the electrons over a wider energy range is easy, while lasers operate in restricted frequency intervals. Additionally, resonant states of all symmetries can be excited, not only the dipole selected states.

Our description of the laser field assumes that the following conditions hold: (i) the number of photons per mode (in our case there is only one mode) of the laser is large so that the field may be treated classically; (ii) the wavelength of the laser is large compared with the spatial extend of the atom so that the dipole approximation is applicable; and (iii) the pulse duration is long compared to typical scattering times. Floquet theory calculates quasistationary solution of time dependent Schrödinger equation (TDSE) for a monochromatic field equation. In the RMF approach, the time-dependent wavefunction is written in a Floquet-Fourier form, so that the TDSE is transformed into a time-independent eigenvalue equation, in which atom-field coupling is treated in a fully non-perturbative manner. This implies that all resonant couplings, as well as non-resonant and high-order laser-induced coupling, are fully accounted for. The laser dresses the autoionizing state, and the projectile electron, and we assumed the following: at resonance this dressing is dominated by the resonant coupling between these states so that we can ignore the influence of the remaining states. Models of this type have been able to reproduce well a variety of *ab initio* calculations of multiphoton

ionization processes involving autoionizing states. The resulting qusienergies are complex with the imaginary part being equal to minus one half times the ionization rate of the state. This represents a quasi-stationary picture in which the atom decays exponentially in time.

The work is structured as follows: Section 2 gives our model for studying the high intensity laser pulse interaction with Li-like Al and C ions. Section 3 presents our procedure for analyzing resonances in laser assisted atomic collision, which exploits the analytic properties of the R-matrix Floquet theory to obtain the intensity dependence of resonance profile. We explore the possibility of using developed two-state model in conjunction with Fano theory in order to investigate intensity dependence of resonance profiles in ultra-short, high intensity laser-atom interaction. Section 4 gives results from the opacity calculation. A general feature of a laser plasma X-ray spectrum is the presence of the so-called satellite lines on the longer wavelengths side of each resonance line. These lines, for which the ion levels involved in the transition are the same as for the corresponding resonance lines, are emitted as a consequence of the dielectronic recombination process. The presence of a further bound electron in an excited state causes the emission to occur at a slightly longer wavelength. Opacity issues are of crucial importance when modeling X-ray spectra from laser-plasmas. Section 5 gives our concluding remarks and future works.

2. NON-PERTURBATIVE TREATMENT OF IONS IN LINEARLY POLARIZED ELECTROMAGNETIC FIELD: THE TWO STATE MODEL FOR LASER INDUCED DEGENERATE STATES (LIDS). APPLICATION TO LITHIUM ISO-ELECTRONIC SEQUENCE

The calculation reported here is part of a general investigation which started with studies of $\Delta n = n' - n = 0$, n, n' ranging from 5 to 12 for C^{2+} and from 9 to 12 for Al^{9+} [24], and $\Delta n = 2$ in Be-like carbon [25]. We only recall here the principal ideas of the theory and the numerical methods. Only the relevant equations will be repeated here. The basic process of interest is as follows:

$$e^- + X^{Z+1}(1s^2 2s(^2S)) \Leftrightarrow X^{Z**}(1s^2 2pn's(^1P)) \xrightarrow{h\nu} X^{Z*}(1s^2 2sn''s(^1S)). \quad (1)$$

In the above equation X^{Z+1} signifies the Li-like ion, of nuclear charge Z, in its ground state, and X^{Z+**} is the doubly excited state of the corresponding Be-like ion of nuclear charge Z. From equation (1) we see that, while radiative transition probability, Γ^r, is approximately independent of n' for high n', the autoionisation width, Γ^a, behaves as $\Gamma^a = \frac{a}{n'^3}$, where a is some constant which depends on the Rydberg series but not on n'. Hence for sufficiently high n' Eq. (1) will hold. In

this case it is necessary to take account of the radiation field in calculating the autoionization process. This means that a simple use of perturbation theory is not appropriate.

The method of procedure is illustrated in Fig. 1. Our approach is to consider the reverse process in the equation (1) corresponding to single-photon ionization. This transition should be studied throughout resonant Rydberg series in a region where the autoionizing and radiative rates are comparable in size. We will consider a laser field of angular frequency $\omega = \Delta E$ (the transition energy corresponding to the initial unperturbed – field free-Rydberg states) and an intensity given (as an appropriate guess) by the electric field strength of the 2s–2p core transition in Li-like ion. It is analyzed the situation when two excited Rydberg states are resonantly coupled by an intense, monochromatic, monomode, linearly polarized laser field. In order to understand the general features of these structures embedded by the field, we have used a model that retains the essential ingredients of the full R-matrix Floquet calculation, namely, a bound state coupled nonperturbatively by the field to an autoionizing state and to the continuum.

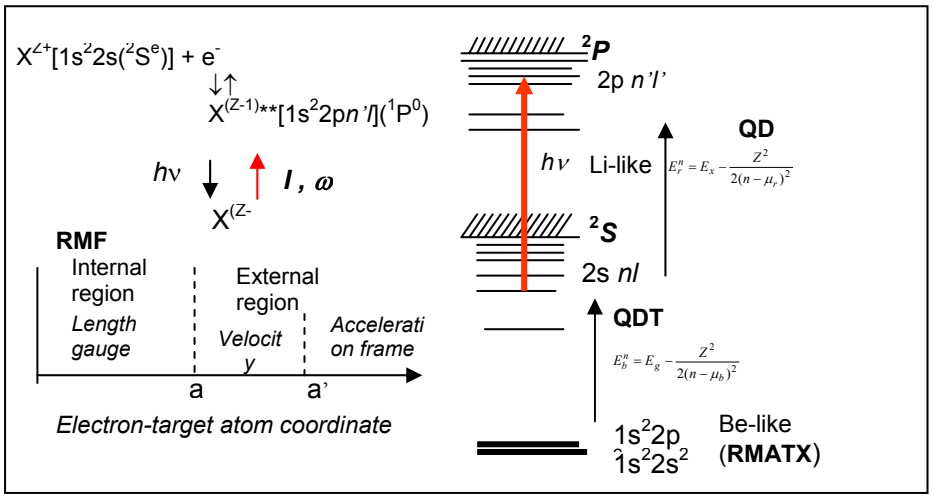

Fig.1 – Resonant single-photon ionization approach.

An initial calculation based on the quantum defect theory (QDT) and the standard R-matrix has been done. This is to calculate the $1s^2 2s^2$ and $1s^2 2p^2$ ground states for Be-like ions in Eq.(1), including full description of the electron-electron correlation and exchange effects. The energies belonging to the corresponding Rydberg excited states $1s^2 2snl$ and $1s^2 2pn'l$ have been evaluated using quantum defect method. The $1s^2 2pn'l$ state energy has been evaluated relative to ^2P ionization threshold while, the energy of the excited 'bound' state $1s^2 2snl$ is evaluated relative to ^2S ionization threshold.

The atomic system was then dressed by a monochromatic mono-mode linearly polarized laser field the intensity of which is given by the field strength of the core transition 2s-2p and the frequency by the energy of the core transition. The laser dresses the autoionizing state, and the projectile electron, and we assume the following: at resonance this dressing is dominated by the resonant coupling between these states so that we can ignore the influence of the remaining states. This represents a quasi-stationary picture in which the atom decays exponentially in time. For two Floquet states, the complex energies as function of the field intensity, I, and frequency, ω, are given in:

$$2E_{1,2} = E_a + E_g - \omega - i\,(\,\Gamma^a + I\gamma)\,/2 \pm \Omega, \tag{2}$$

$$\Omega = \{[d - i(\Gamma^a - I\gamma)/2]^2 + \Gamma^a\, I\gamma[q - i]^2\}^{1/2}.$$

In the equations (2) γ is the coupling parameter of the "ground" state to the unstructured continuum and q is the Fano line profile index for resonance transition. The two-state model [22, 23] qualitatively reproduces the behavior of the Floquet states, showing that the coupling via the continuum is more important than the direct dipole coupling between states. E_g is the zero-field position of the ground state on the real energy axis, while the energy of the autoionizing state is shifted by –ω. Thus the zero-field position of the autoionizing state changes with ω, being scaled at the complex energy $-\omega + E_a - i\Gamma^a/2$, where Γ^a is the field-free width of the autoionizing state. The corresponding detuning is defined as $d = E_a - E_g - \omega$.

We illustrate the method studying the motion of the complex energies in the complex plane as function of the field intensity for different field frequencies and atomic parameters. Most interesting is the critical region where a crossing (or an avoiding crossing) of trajectories occurs.

Figure 2(a, b) reproduces the motion in the complex plane of trajectories belonging to the 'bound' and the excited Rydberg states in C^{2+}. Fig. 2a gives the motion in the complex plane of the complex energies belonging to $1s^2 2s5s$ (^1S) (denoted by 'b') and $1s^2 2p5s(^1P^0)$ (denoted by 'r') states as function of frequency and field intensity. Corresponding curves have the same line type (solid or dashed). The field intensity is varied from 0.0 to 10^{13} W/cm^2. Fig. 2b gives trajectories of the complex energies belonging to $1s^2 2s7s(^1S^e)$ and $1s^2 2p7s(^1P^0)$ states, for frequencies 0.2987 and 0.2989 atomic units. The intensity is varied from 0.0 to 10^{12} W/cm^2.

The 2-state model has two LIDS points at particular frequencies and intensities. Close to these points, LIDS frequency for fixed intensity, can be predicted as complex trajectories with a real part avoided crossing and an imaginary part crossing switch to having a real part crossing and an imaginary part avoided crossing as ω passes through LIDS frequency. For certain values of field's intensity and frequency, the two quasi-energies become equal, giving rise to laser-induced degenerate states (LIDS).

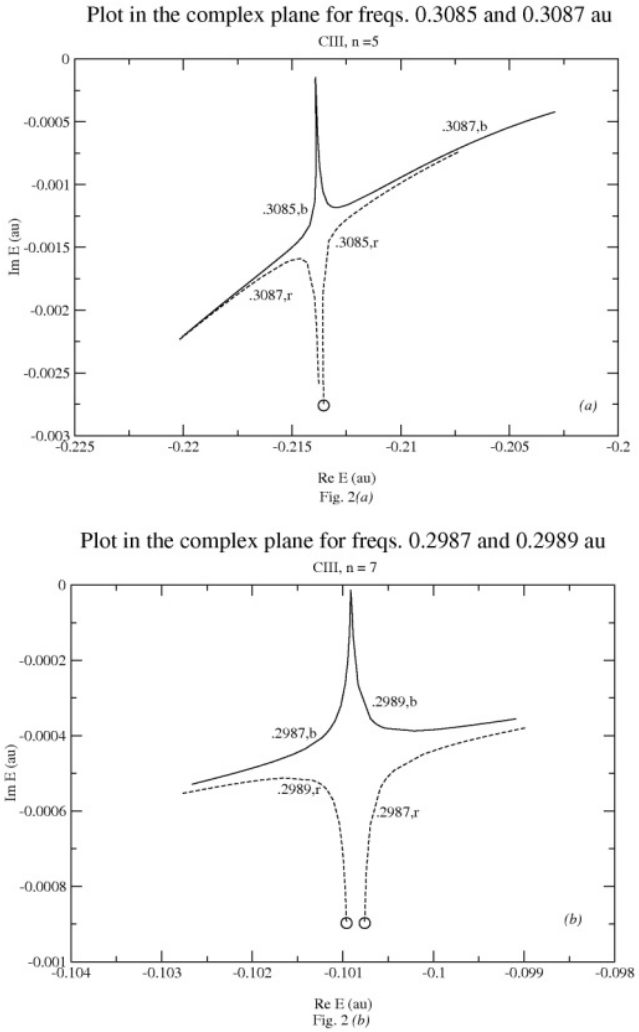

Fig. 2 – *a*) Trajectories of the complex energies of $1s^2 2s5s(^1S^e)$ $1s^2 2p5s(^1P^0)$ states in C^{2+}, for frequencies 0.3085 and 0.3087 atomic units. The intensity is varied from 0.0 to 1.10^{13} W/cm^2; b) trajectories of the complex energies of $1s^2 2s7s(^1S^e)$ and $1s^2 2p7s(^1P^0)$ states in C^{2+}, for frequencies 0.2987 and 0.2989 atomic units. The intensity is varied from 0.0 to 1.10^{12} W/cm^2.

In all curves where we are really close to the LIDS position, the imaginary part of the bound state energy, i.e. the width, increased rapidly with intensity while, the real part remained essentially constant. Also, the width of autoionizing state decreased rapidly from its zero field value and its real part of the energy also remained essentially constant. Therefore if the equivalent intensity of the spontaneous emission is less than the LIDS intensity then the two widths are converging towards each other into the region where perturbation theory should not be used.

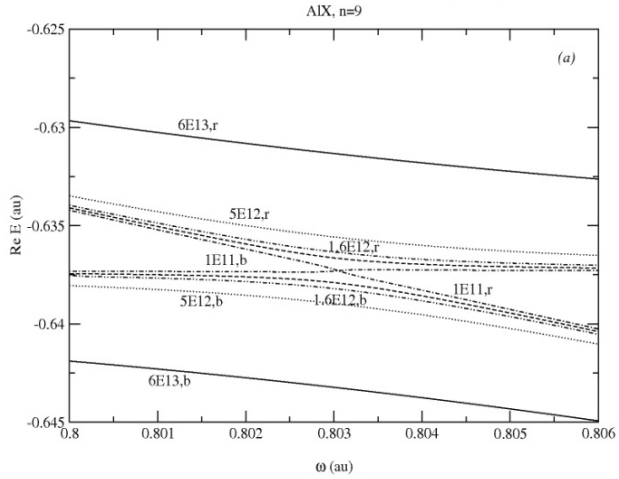

a)

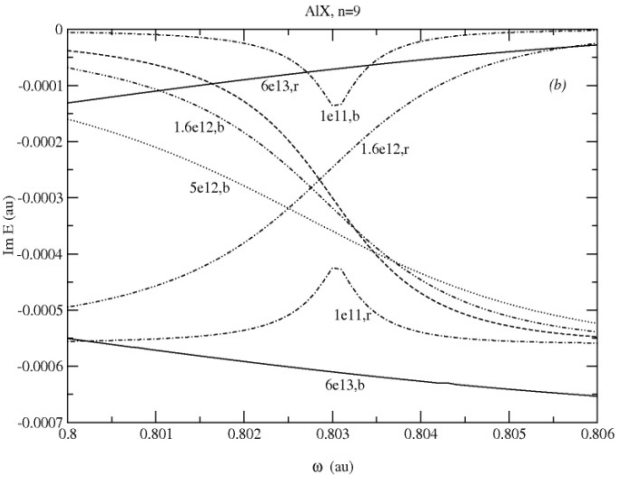

b)

Fig. 3 – *E* as function of frequency: a) real part of *E* as function of frequency, in atomic units, for given intensities, corresponding to 2sns($^1S^e$) and 2pns($^1P^0$) states with $n = 9$ in AIX. The curves have solid and dashed lines and are labeled as 'b' and 'r', respectively. Corresponding intensities are indicated next to the curves. b) imaginary part of *E* as function of frequency, in atomic units, for given intensities, corresponding to 2sns($^1S^e$) and 2pns($^1P^0$) states with $n = 9$ in AIX.

In Figure 3(a, b) we reproduce the behavior of the real and imaginary part of the complex energies at fixed field intensity, as function of the field frequency. Fig. 3a shows the real parts of *E* as function of frequency, in atomic units, for given intensities, corresponding to 2sns($^1S^e$) and 2pns($^1P^0$) states with $n = 9$ in Al X. The curves have solid and dashed lines and are labeled as 'b' and 'r', respectively.

Corresponding intensities are indicated next to the curves. In Fig. 3b are given the corresponding imaginary parts of E as function of frequency, in atomic units, for given intensities.

At weak intensity there is a clear evidence of the interference between the two resonant Rydberg states (the first crossing). As the intensity of the field is increased the crossing of the imaginary parts of the quasi-energies which correspond to the 'ground' Rydberg state apparently ceases to exist.

At lower intensity ($1.5\ 10^{12}$ W/cm^2 Al X) the RMF calculations show a dip in the width of the 'ground' state at frequency about 0.803 a.u. These minima become exact zero if the ratio of the squared dipole matrix elements coupling these states to the continua tends to zero. The energies of the Rydberg states are shifted by $-\omega$, where ω is the laser frequency. Away from the resonances, the curves correspond to the 'ground' Rydberg state and the 'resonant' Rydberg state, respectively. At low intensity, the avoided crossings are well separated, whereas this is not the case at the higher intensity where we see that the separations of the avoided crossings are comparable to the energy separation of the two Rydberg states [26]. The first demonstration of $\Delta n = 2$ radiative transition has been done by Stancalie [25]. Figure 4 presents these results for comparison with those obtained for $\Delta n = 0$.

3. INTENSITY DEPENDENCE OF RESONANCE PROFILES IN ULTRA SHORT, HIGH INTENSITY LASER-ATOM INTERACTION

The intensity-dependent behavior of the resonance profiles is closely related to the proximity of LIDS. We have derived a simple model to describe the structure of this degeneracy. From this model one may ascertain the effect of LIDS upon the resonance absorption profile in the photodetachment rate of the ground state of the model ion. The description generalizes the non-radiative coupling matrix element of the autoionizing state to the continuum, so as to include an explicit intensity dependence. The process under investigation is described within the general theory on double poles of the S matrix occurring in laser-assisted electron-scattering by an atom in the neighborhood of an autoionizing resonance with a quasibound state of the composite electron-atom system. For 'capture-escape' resonance, the Breit-Wigner expression for corresponding cross section is:

$$\sigma(E, I, \omega) = \frac{2\pi g}{E} \frac{\frac{1}{2}\Gamma_g}{\left(E - E_g - \omega\right)^2 + \frac{1}{4}\Gamma_g^2}. \tag{3}$$

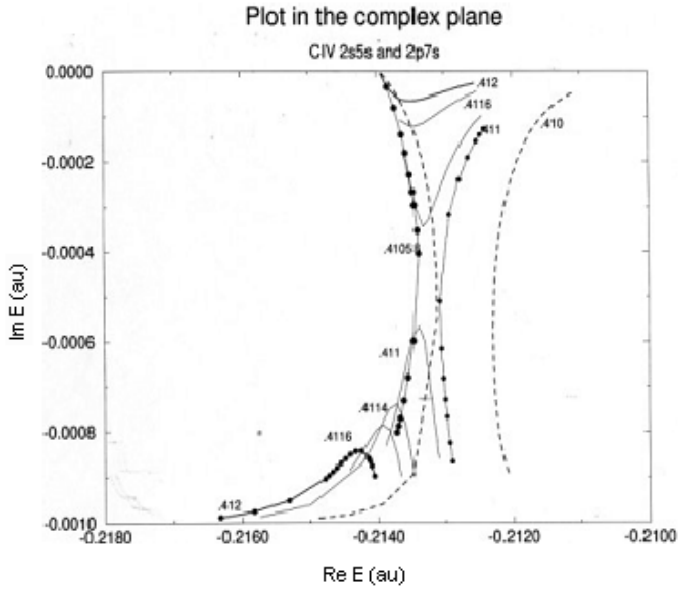

Fig. 4 – Trajectories of the complex energies of $1s^2 2s5s(^1S^e)$ and $1s^2 2p7s(^1P^0)$ states as function of field intensity and frequency. For each frequency, there are two curves, one connected adiabatically to the 'bound' and the other to the autoionizing state. The intensity is varied from 0.0 to 5.10^{13} Wcm^{-2}. The small dots give intensity in steps of 5×10^{11} W cm^{-2}. At very small detunings (e.g. ω = 0.412au), the curve connected to the autoionizing state increases in width with intensity, while the bound state is "trapped" closed to the real axis. For intermediate detunings, two structures are visible, about which the curves of the 'bound' states and of the autoionizing state exchange their roles. The atomic units are used and the energy scale is chosen such that ground states energy is set to zero.

This quantity becomes zero for a particular value of the electron energy $E(I,\omega)$ at which the dipole coupling between the ground state and the autoionizing state is zero. Intensity-dependent shifts of the position E_g are small at frequencies and intensities considered in these calculations and are therefore ignored. A simple model has been developed [27] so as to reinforce the role of Laser Induced Degenerate State phenomenon on resonances obtained by laser. Table 1 gives the calculated widths of the qusienergies at the first LIDS positions. The effect of constant ratio in Table 1 is to produce a resonance profile that becomes narrowed and taller, then wider and lower as laser field intensity increases. When only a single resonant process occurs, either in the limit that the laser intensity goes to zero so that only the autoionizing resonance remains, or in the limit that the width of the autoionizing state goes to zero, leaving only the 'capture- escape' resonance, the ratio of the scattering cross section to the background cross section reduces to the Fano line shape formula. The Fano resonance formula is algebraically simple. A dimensionless energy ε is used to measure energy differences from a resonance energy E_r in terms of the half-width.

Table 1

The calculated widths, Γ, in atomic units *(au)*, at the first LIDS positions in C^{3+}. The principal quantum numbers, n, describes both, 'bound' and 'excited' Rydberg states of type $1s^2 2sns(^1S)$ and $1s^2 2pns(^1P)$ respectively, embedded by the electric field

n	$2n^3\,\Gamma$(au)
5	0.17
6	0.15
7	0.15
8	0.15
9	0.15
10	0.15
11	0.14
12	0.16

For an *isolated* autoionization state with a resonant width Γ at resonant energy E_r, the resonant structure can be described in terms of the asymmetry parameter q. This parameter is a measure of the importance of the direct transition from the ground to the continuum compared to transition via the autoionizing state. High q means weak direct transition and symmetric line shape since the interference is minimized. Qualitatively, the q parameter measures the interference between transitions from the initial state to the bound and continuum components of the final-state wave function. If the resonance is dominated by the contributions from the transitions to both bound and continuum components of the final-state wave function, its corresponding q value is generally large and the resonant feature is approximately symmetric. If the contributions from transitions to bound and continuum components of the final-state wave function are comparable, the resonant structure is asymmetric with an intermediate q value. If the spectrum is strongly dominated by the transition to the continuum component of the final-state wave function, a *window resonance* with zero cross section is expected either at or near the resonant energy E_r with $q \to 0$.

In Fig. 5 the ratio $R = (q+\varepsilon)^2/(1+\varepsilon^2)$ is plotted as function of relative energy parameter and different q values for the $1s^2 2pns(^1P^0)$, $n = 5$ state in CIV. The relative energy has been determined as $\varepsilon = \left[2(E_g + \hbar\omega - E_a \right]/(\Gamma_a + \gamma_a - \Gamma_g)$, where E_g, ω, and E_a are, respectively, the field free position of the excited Rydberg state, the tuning frequency and the field-free position of the autoionizing state, as output from the R-matrix Floquet calculation.

Preliminary results on intensity dependence of the line profile have been obtained based on the eigenphase fitting procedure. The method uses R-matrix theory to determine the energy variation of the eigenphase analytically rather than numerically. Fitting the energy dependent K-matrix directly is difficult because K has a pole in the resonance region. Therefore it is easier to fit the arctan (K). Following this method, the eigenphase derivative is a well behaved function of E near the resonance.

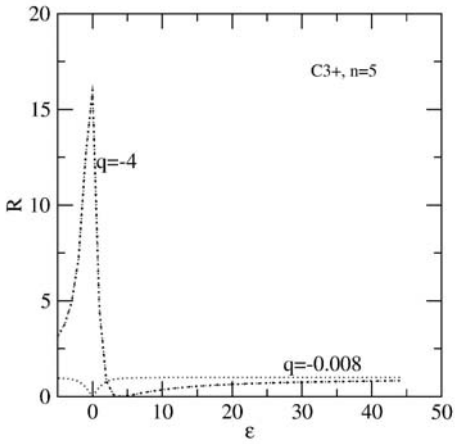

Fig. 5 – Line profile ratio for $1s^2 2p5s\ (^1P^0)$ resonant state in C IV, as function of the relative energy parameter (a.u.)

A scaling relation has been obtained as function of the effective quantum number [27]. Figure 6 shows the 'scaled' width dependence of the autoionizing width with the 'bound' excited Rydberg state effective quantum number (υ_1).

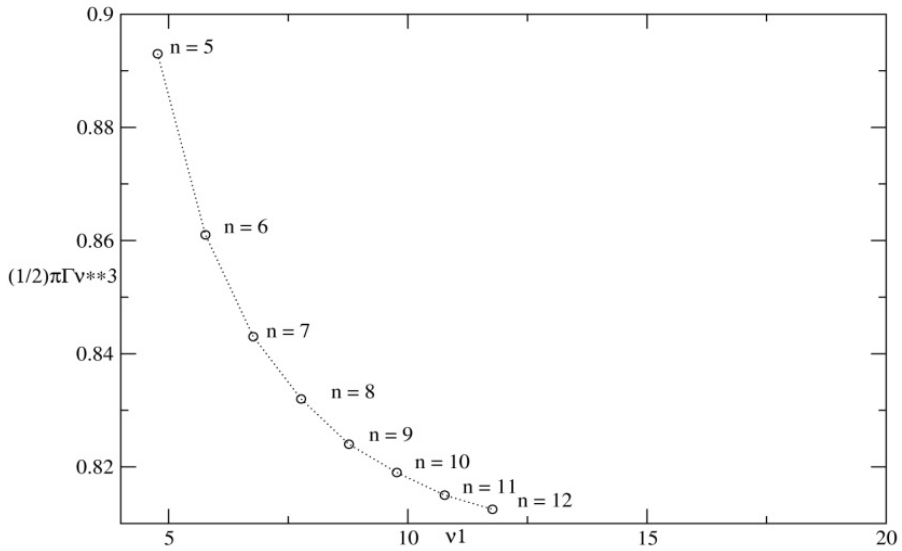

Fig. 6 – The 'scaled' width dependence of the autoionizing width with the 'bound' excited Rydberg state effective quantum number(υ_1).

Denoting $\Gamma^{r,n}$ radiative width in the channel n, where $\Gamma^{r,n} = I / \omega_n$, ω_n being LIDS frequency, we have obtained usual scaling relation $\Gamma^{r,n\ (CIII)} / \Gamma^{r,n(ALX)} = 11/4$.

Corresponding relation for autoionization widths is $\Gamma^{a,n\ (CIII)}/\ \Gamma^{a,n(ALX)} = 1.4 = (11/4)^{1/3}$. Finally, the branching ratio $B^{n,\ CIII} = \Gamma^{r,n\ (CIII)}/\Gamma^{n,\ LIDS} = 0.986/n^3$ and $B^{n,\ ALX} = \Gamma^{r,n\ (ALX)}/\Gamma^{n,\ LIDS} = 0.306/n^3$, which corresponds to a scaled relation on Z as $B^{n,\ CIII}/\ B^{n,\ ALX} = 1/3$.

4. PLASMA OPACITY EFFECT ON THE LINE RADIATION

Modeling of the plasma, requiring collisional and radiative processes to perform calculation on population densities, ion abundances, line radiation or radiated power has basically been performed with the aid of Atomic Data and Analysis Structure (ADAS) package which is an interconnected set of computer codes and data collections for assisting in the analysis and interpretation of spectral measurements. Its structure has interactive and non-interactive capabilities. The interactive part provides immediate display of important fundamental and derived quantities used in analysis together with a substantial capability for exploring parameter dependencies and diagnostic predictions of atomic population and plasma models. The second part is non-interactive but provides a set of subroutines which can be accessed from the user's own codes to draw in necessary data from the derived ADAS database.

Experimental and theoretical determinations of the radiative opacity have long been of interest. Many physical effects which have been treated approximately or ignored in theoretical models may affect the accuracy of opacity. Some discrepancies are supposed to be a consequence of line saturation effect. We have derived atomic data for opacity model including the contribution of the bound-free and bound-bound transitions. The model is based on escape factor approximation [28].

In laser-produced plasmas, photons due to radiative transitions from the lower level of an X-ray lasing transition to a lesser-energy level of the same ion may repopulate the former and destroy the population inversion, leading to an attenuation of the gain. This effect is called photon reabsorption or radiation trapping. In our model reabsorbed photons originate from resonance transition between the lower lasing level and the ground level. The variation of lower lasing level population yields a corresponding variation for all levels of the lasing ion, with regard to spontaneous emission, collisional excitation and de-excitation. Simulating the effect of opacity on quantum state populations and emission of radiation from plasma is often made with a hydrodynamic code coupled to atomic physics code. These calculations can be made using different methods and computer codes more or less complicated. One such atomic data and program package is ADAS. Due to re-absorption the escape intensity from the plasma is less

than the integrated emission along the line of sight. A secondary effect is that the population distribution of the absorbing atom or ion state could be altered. Line ratios are function of electron temperature and density, but also of opacity.

We have calculated the escape population factor and the escape intensity factor for the lasing transition $3d_{5/2}$-$4f_{7/2}$ of Li-like Al. An initial atomic data calculation for fine structure levels have been done using the R-matrix method [29,30]. These data were included in the ADAS codes to calculate population density distribution on the excited levels including those for which X-ray radiation has been experimentally measured [31].

The normalized population escape factor is presented in Fig. 7 as function of the optical depth. The modified line intensity profile is shown in Fig. 8.

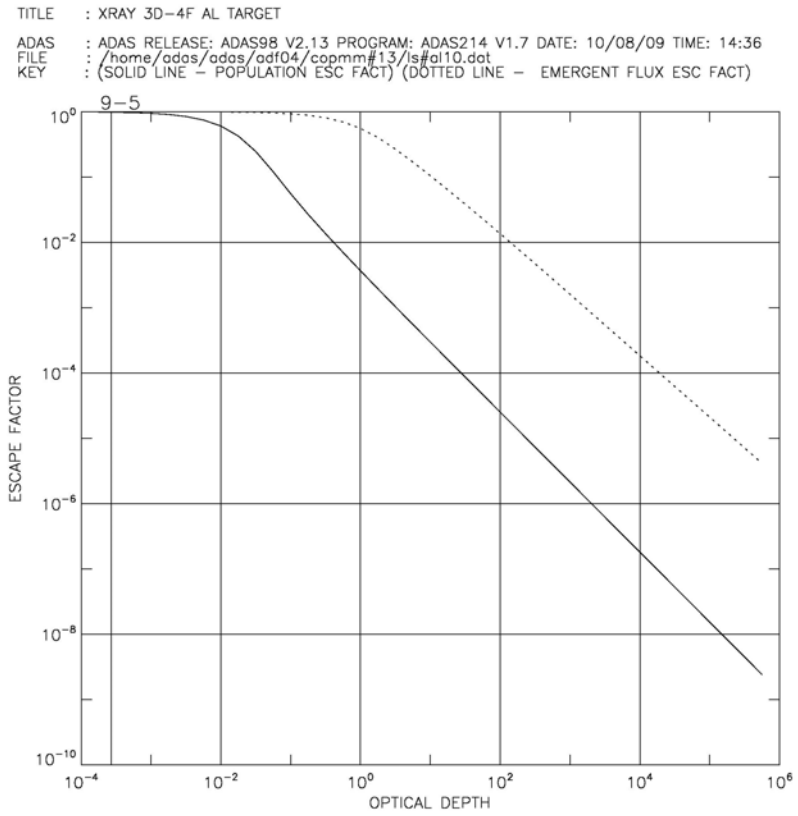

Fig. 7 – Normalized population escape factor for lasing transition $3d_{5/2} - 4f_{7/2}$ in Li-like Al.

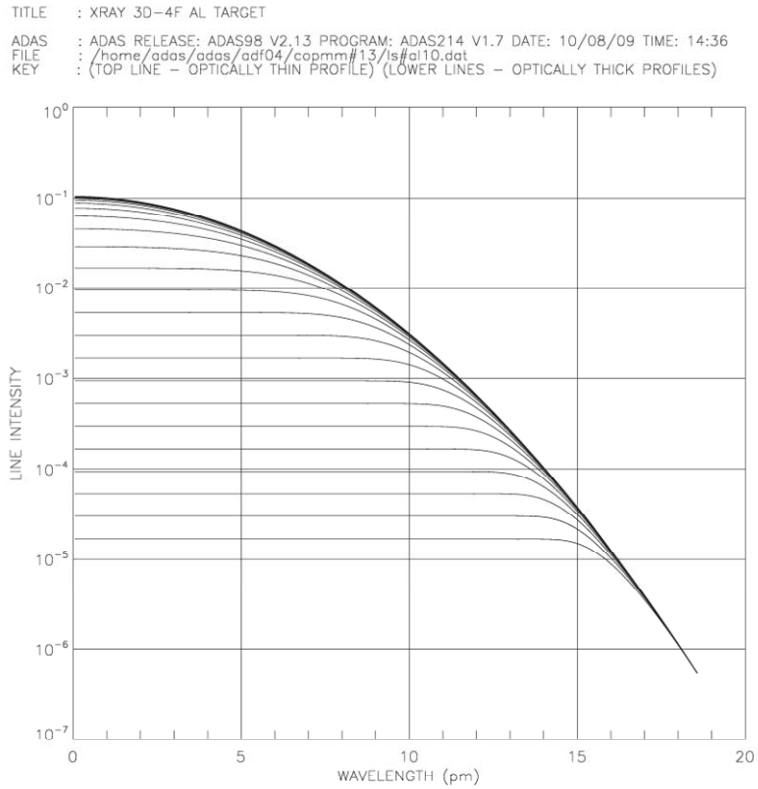

Fig. 8 – The modified intensity line profile for lasing transition $3d_{5/2} - 4f_{7/2}$ in Li-like Al.

5. CONCLUDING REMARKS

In this work we summarized partial results from theoretical modeling of the interaction of high intensity laser radiation with atoms and plasmas. Laser-atom interaction has been studied in connection with degeneracy and population trapping. Laser-plasma interaction has been considered from the point of view of relations between photon emission rate and ionization or recombination flux which contribute to the opacity effects.

The simulation of the effects of the relativistic electron beam produced by the laser requires the modeling of the electron source and the transport of relativistic electrons in high-density materials. We have compare the effective collision strengths produced by electrons [32] and protons [33] in a laser produced plasma on aluminum target irradiated by a laser wavelength $\lambda = 1.06$ μm, pulse duration 120ps and intensity 2.31 10^{13}W cm^{-2}. Our results provide a firm foundation on

which larger calculations may be based. From our model one may ascertain the effect of LIDS upon the resonance absorption profile in the photo-detachment rate of the ground state of the model ion. We expect that the autoionization of the lower doubly-excited level will remove the constraint on the size of the probe-pumped plasma that is imposed by radiation trapping in other photo-pumping schemes. The alternative pumping scheme promising possibility to dramatically reduce pump power requirements has important implications for the next generation of plasma lasers. Essentially, it breaks the symmetry between absorption and stimulated emission by using a coherent laser whose frequency closely matches the transition between the upper level and some other auxiliary level. The lasing medium can be coherently prepared in such a way that absorption between the lower and upper levels is reduced or eliminated. The theoretical mechanism for this process is quantum mechanical interference between two different paths leading to the excited state. This scheme involves two close-lying autoionizing (AI) states as upper operating levels. The gain in this scheme can be rather large if the two selected AI states satisfy the following conditions: (a) they decay into the same continuum, (b) one or both AI states have large Fano parameters, and (c) the spacing between these levels is comparable with their autoionizing widths. This phenomenon is called 'electromagnetically induced transparency' and the theoretical investigative calculation is in progress.

Acknowledgements. Financial support under the *National Authority for Scientific Research* coordinated program **LAPLAS PN 09 39** is gratefully acknowledged.

REFERENCES

1. D. Strickland and G. Mourou, *Compression of amplified chirped optical pulses*, Opt. Commun., 56, 219 (1985).
2. M. Gavrila ed., *Atoms in Intense Laser Fields*, Adv. At. Mol. Opt. Phys. Suppl., **1** (1992).
3. K. Burnett, V.C. Reed and P.L. Knight, J. Phys. B, **26**, 561 (1993).
4. C. J. Joachain, *Theory of laser-atom interactions, in: Laser Interactions with Atoms, Solids and Plasmas*, R.M. More, ed. Plenum Press, New York, 1994, p. 39.
5. L.F. DiMauro and P.Agostini, Adv. At. Mol. Opt. Phys., **35**, 79 (1995).
6. M. Protopapas, C.H. Keitel and P.L. Knight, Rep. Progr. Phys., **60**, 389 (1997).
7. G. Malka, E. Lefebre, and J.L. Miguel, Phys. Rev. Lett., **78**, 3314 (1997).
8. D. Bauer, P. Mulser, and W. –H. Steeb, Phys. Rev. Lett., **75**, 4622 (1995).
9. P.Mora and T.M. Antonsen Jr., Phys.Rev. E, **53**, R2068 (1996).
10. S G Rykovanov et al. New J. Phys., **10** (2008)113005 and references herein.
11. P.L. Knight, Comments on Atomic and Molecular Physics, **15**, 193 (1984).
12. N.J. Kylstra, E. Paspalakis, P.L.Knight, J. Phys. B, **31**, L719 (1998).
13. YL Shao, O. Faucher, J. Zhang, D. Charambidis, J. Phys. B, **28**, 755 (1995).
14. Fursa D V and Bray I, Phys. Rev. A, **52**, 1279 (1279).
15. Cartwright D C and Csanak G, Phys. Rev. A, **38**, 2740 (1988)

16. D.C. Griffin, M.S. Pindzola, F. Robicheaux, T.W. Gorczyca, and N.R.Badnell, Phys. Rev. Lett., **72**, 3491–3494 (1994).
17. Bartschat K and Madison D H, J. Phys. B, At. Mol. Opt. Phys., **21**, 153 (1988).
18. P.G. Burke and K.A. Berrington, *Atomic and Molecular Processes: an R-matrix Approach*, IOP Publishing, Bristol, 1993.
19. Bartschat K, Hudson E T, Scott M P, Burke P G and Burke V M, JPB, **29**, 115(1996); PRA **54** R998 (1996); JPB, **29**, 2875 (1996).
20. P.G. Burke, P. Francken and C J Joachain, Europhys. Lett., **13**, 617 (1990).
21. P.G. Burke, P. Francken and C J Joachain, J. Phys. B, **24**, 761 (1991).
22. O. Latinne, N.J. Klistra, M. Dörr, J. Purvis, M. Terao-Dunsheath, C.J. Joichain, P.G.Burke, C.J.Noble, Phys. Rev. Lett., **74**, 46 (1995).
23. A.Cyr, O. Latinne and P.G. Burke J. Phys. B, **30**, 659 (1997).
24. V. Stancalie. Physics of Plasmas, **12**, 043301 (2005)
25. V. Stancalie, Physics of Plasmas, **12**, 10075 (2005).
26. V. Stancalie V , Laser and Particle Beams, **27**, 345 (2009).
27. V. Stancalie, Nuclear Instruments and Methods in Physics Research Section B: Beam Interactions with Materials and Atoms, Vol. 267, 305 (2009).
28. V. Stancalie, E. Rachlew, Physica Scripta, **66**, 444 (2002).
29. V. Stancalie, V. M. Burke, A. Sureau, Phys. Scr., **59**, 52 (1999).
30. V. Stancalie, Phys. Scr., **61**, 459 (2000).
31. V. Stancalie *et. al.*, in *Laser Interaction with Matter*, IOP Conference, Series **140**, 133 (1995), S.Rose Ed.
32. V. Stancalie, V. Pais, Laser and Particle Beams, **24**, 235 (2006).
33. V. Stancalie, V. Pais, M. Totolici, A. Mihailescu, Laser and Particle Beams, **25**, 267 (2007).